

Li⁺- and H⁺-Exchanged Low-Silica X Zeolite as Selective Nitrogen Adsorbent for Air Separation

Jin-Bae Kim

Department of Chemical Engineering, Hoseo University, Asan-city, Choongnam 336-795, Korea

Received August 11, 2003

Li⁺ and H⁺ co-exchanged LSXs (Li-H-LSX) with various ratios of Li⁺ and H⁺ were prepared, and those adsorption characteristics of nitrogen and oxygen were compared with Li-Na-LSX and Li-Ca-LSX. Li-H-LSX showed higher nitrogen capacity and selectivity than that of Li-Na-LSX in the wide range of Li-exchanged ratio. The nitrogen capacity of Li-Ca-LSX was slightly higher than that of fully Li- or Ca-exchanged LSX (Li-LSX or Ca-LSX). However, Li-Ca-LSX showed low nitrogen/oxygen adsorption selectivity until the Li content reached about 80%, which was a tendency near that of Ca-LSX.

Key Words : Low-silica X zeolite, Ion-exchange, Selective nitrogen adsorption

Introduction

Production of oxygen by pressure swing adsorption (PSA) applies to the property in which nitrogen having higher quadrupole moment than oxygen can be selectively adsorbed into the pore of zeolite. Since the PSA method can produce the oxygen at a low cost, it has come into wide use industrially. The nitrogen adsorption capacity and selectivity could be affected by the framework structure, Si/Al ratio, the kinds of cations corresponding to the framework aluminum, and so on. Minato et al. reported that the cation with higher surface charge density showed higher adsorption capacity for nitrogen and carbon dioxide.^{1,2} Ca-exchanged A zeolite (Ca-A) was initially used as conventional adsorbents in PSA processes for oxygen production.

In the early 1980s, PSA process was improved by adopting a vacuum pump for regeneration of adsorbent, and it is called pressure vacuum swing adsorption (PVSA). In the PVSA system, the difference in the performances of adsorbents became more remarkable. The adsorbent was also improved with improvement of system. A zeolite has a small pore structure with 8 oxygen-ring openings made up of a cubic arrangement of sodalite cages linked through double 4 oxygen-rings. X zeolite has a large pore structure with 12 oxygen-ring openings made up of sodalite cages linked through double 6 oxygen-rings. Therefore, X zeolite has more advantages as adsorbent than A zeolite. Having high capacity and selectivity of nitrogen, Ca-exchanged X zeolite (Ca-X) has been widely used for the PVSA system after the 1980s.

Since the number of ion-exchange sites working as adsorption sites of commercial X zeolite with Si/Al ratio of about 1.2 is fewer than that of A zeolite with Si/Al ratio of 1.0, a structural merit of X zeolite could not be fully utilized. However, X zeolite with Si/Al ratio of 1.0, called low silica X (LSX) zeolite, can also be synthesized by hydrothermal

method, and it was known as outstanding nitrogen adsorbent.³

On the other hand, Li-exchanged X zeolite (Li-X) was proposed as a high performance adsorbent for production of oxygen.⁴⁻⁸ In particular, Li-exchanged LSX zeolite (Li-LSX) has remarkable nitrogen adsorption capacity and selectivity. Recently, Li-LSX has been considered to be the best adsorbent for oxygen PSA.⁶⁻¹³ However, the higher Li-exchange ratio should be required to prepare the Li-LSX with high performance to oxygen producing by P(V)SA.^{6,7,12} Compared with the other available cations for selective nitrogen adsorption like Ca, Li source is expensive and it was reported that the Li ions are hard to be exchanged to X zeolite.¹⁴ To reduce the usage of Li ions, many researches, such as introduction of second and/or third cations and Li recovery from waste solution of ion-exchange treatment, were conducted.¹⁵⁻¹⁸ It was reported that some second cations like Ca and Sr were effective in reducing the Li ratio without decrease in adsorption performance.^{15,16} Yoshida *et al.* reported that the nitrogen adsorption capacities of Li-exchanged FAU type zeolites such as LSX, X and Y is related to the location of Li ions in FAU structure.^{12,13}

In this study, ammonium ions were introduced as second cation. The ammonium ions were transformed into proton by desorption of ammonia with calcinations. Finally, Li⁺ and H⁺ co-exchanged LSXs (Li-H-LSXs) with various ratios of Li⁺ and H⁺ were prepared, and those adsorption characteristics were compared with Li-Na-LSX and Li-Ca-LSX.

Experimental Section

LSX crystalline powder was synthesized by hydrothermal method. The ingredients of LSX were NaOH (Daiso, 48% solution), KOH (Daiso, 85%), sodium silicate solution (Daiso, 29 wt% SiO₂-9.5 wt% Na₂O-61.5 wt% H₂O), sodium aluminate solution (Asada, 20 wt% Al₂O₃-19 wt% Na₂O). The chemical composition of precursor gel was 1.00 Al₂O₃-1.75 SiO₂-4.28 Na₂O-1.42 K₂O-114 H₂O. Sodium aluminate solution, NaOH, KOH, and H₂O were mixed at first, and

*Phone: +82-41-540-5757; Fax: +82-41-540-5758; e-mail: jbkim@office.hoseo.ac.kr

then the mixture was cooled down to room temperature. Sodium silicate solution was added to the mixture with stirring. The mixed gel was heated at 40 °C in a Teflon container for 15 hours, heated up to 60 °C at a heating rate of 4 °C/hour, and then maintained at 60 °C for 4 hours. After that, the resulting solid products were filtered, and washed with distilled water until the pH of washing water reached below 10.0. The resulting powder was then dried at 100 °C for one night.

The powder of 1.0 g was treated with 1 M LiCl-NH₄Cl mixed solution of 50 mL 5 times repeatedly at 100 °C for 1 hour. The pH of mixed solution was adjusted to 9.0 by addition of LiOH. The resultants were excessively washed with hot distilled water and dried at 100 °C for one night, followed by calcination in a dry air stream at 400 °C for 1 hour. The ratio of Li⁺ and H⁺ was controlled by mixed ratio of LiCl and NH₄Cl in the ion-exchange solution.

X-ray diffraction (XRD) analysis was carried out using a Rigaku RAD-2B with Ni-filtered monochromatic CuK α radiation. For measuring of d_{111} -spacing value, α -alumina powder was used as an internal standard. The morphology of LSX particles was observed with a scanning electron microscope (HITACHI S-570). ²⁹Si MAS NMR spectra were registered using a Jeol JNMGS-270 spectrometer at 53.54 MHz, and tetramethylsilane (TMS) was used as external standard shift reference. The chemical analyses of LSX samples were performed by an inductively coupled plasma spectrometer (Shimadzu, ICPS-1000 III). BET surface area and nitrogen/oxygen adsorption isotherms were measured using a BELSORP 28SA.

Results and Discussion

XRD pattern of as-synthesized LSX showed a typical FAU structure as shown in Figure 1. It is considered from the XRD pattern (Figure 1) and high BET surface area of 716

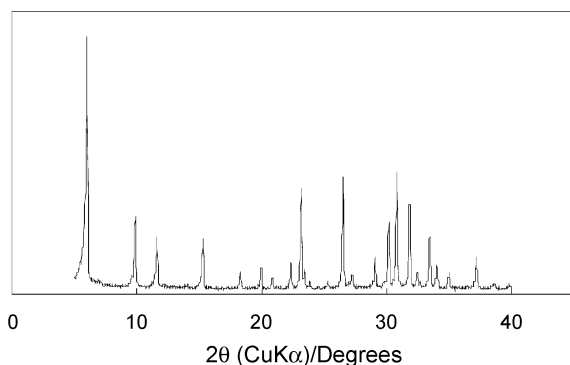


Figure 1. XRD pattern of as-synthesized LSX.

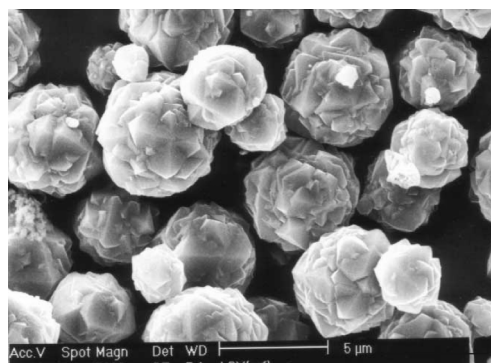


Figure 2. SEM image of as-synthesized LSX.

m²/g (Table 1) that finely crystallized LSX was obtained. SEM image of as-synthesized LSX crystalline powder was shown in Figure 2. The crystal size of LSX was 2-5 μm. Chemical composition of the as-synthesized LSX was similar to that of precursor gel as shown in Table 1. ²⁹Si MAS NMR showed a single resonance at about -86 ppm, which was corresponded to the Si(OAl)₄ group in the zeolite.^{19,20} These results indicate that the LSX prepared in this study has high crystallinity and framework Si/Al ratio near 1.0.

Figure 3 shows nitrogen and oxygen adsorption isotherms at 20 °C of fully Li-exchanged and Ca-exchanged LSX. Although nitrogen capacity of Li-LSX was lower than that of Ca-LSX in the low pressure, it was reversed in the high pressure above 500 torr. The high nitrogen adsorption capacity of Ca-LSX in the low pressure range could be explained by the effect of surface charge density of cations in the zeolite on the adsorption capacity.^{1,2} Shen *et al.*²¹ reported that the primary adsorption heat for nitrogen on Ca-exchanged zeolite was also higher than that of Li-exchanged zeolite. Since the number of cations in the fully exchanged Ca-LSX is the half of Li-LSX, the upward tendency of nitrogen adsorption amount accompanying a pressure rise in the Ca-LSX became small rapidly. These adsorption patterns have strong influence to a performance of PSA for oxygen generation. That is, in PSA operated by pressure change in the predetermined range, the performance is decided by the difference of the adsorption amount in that pressure range. Also in the same pressure range, Li-LSX has higher amounts of nitrogen adsorption used effectively than that of Ca-LSX. Since there was smaller amount of oxygen adsorption than Ca-LSX, Li-LSX is excellent also in selectivity of N₂/O₂ adsorption.

On the other hand, it was reported that the adsorption amount of nitrogen to Li-LSX changed strangely by the Li-exchanged ratio.^{6,12,15} In Li-Na-LSX, nitrogen adsorption

Table 1. Chemical and Physical properties of as-synthesized LSX

Sample	Chemical analysis (molar ratio)			BET surface area (m ² /g)	²⁹ Si MAS NMR
	Si/Al	Na/Al	K/Al		
Na-K-LSX	0.98	0.73	0.30	716	Only one peak around -86 ppm

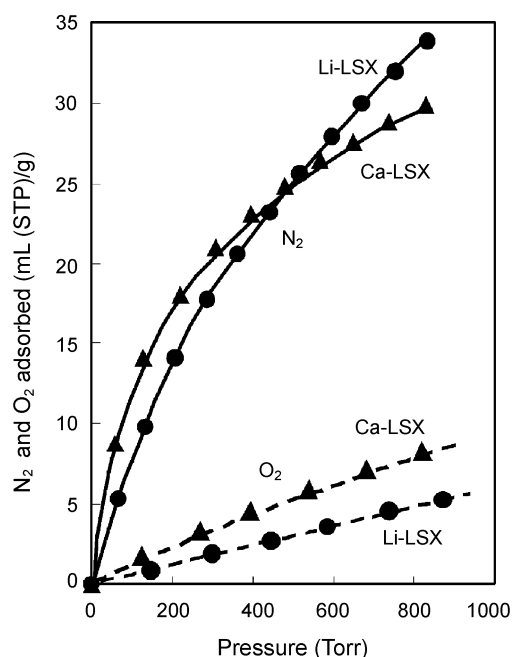


Figure 3. N_2 (solid line) and O_2 (broken line) adsorption isotherms of Li-LSX (●) and Ca-LSX (▲) at 20 °C.

amount did not increase until the Li-exchanged ratio reached 2/3 of total ion-exchange sites as shown in Figure 4. Yoshida *et al.*¹² explained that the specific adsorption behavior of Li-LSX was concerned with the three types of ion-exchange sites in the FAU structure. They suggested that the Li ions are preferentially arranged in a sequential order of site I', site II and site III of FAU structure, and the only Li ions located in site III contributed to adsorption.¹²

Figure 4 shows the change in the amount of nitrogen adsorbed with increase in Li content. The amount of nitrogen adsorbed and the Li content were expressed as the number of nitrogen molecules adsorbed and the number of

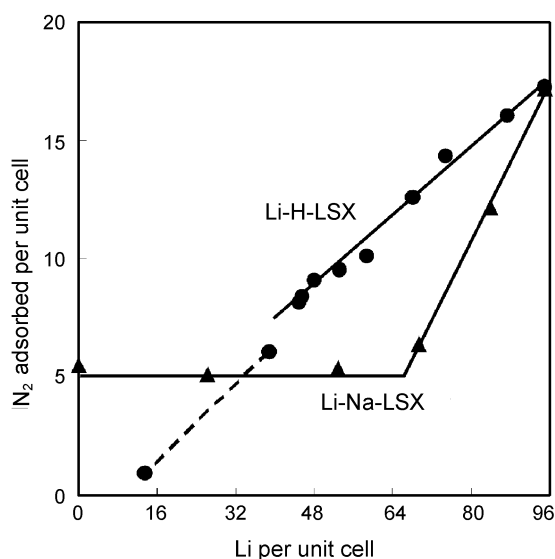


Figure 4. Change in the amount of nitrogen adsorbed by Li content in Li-H-LSX (●) and Li-Na-LSX (▲) at 760 torr, 20 °C.

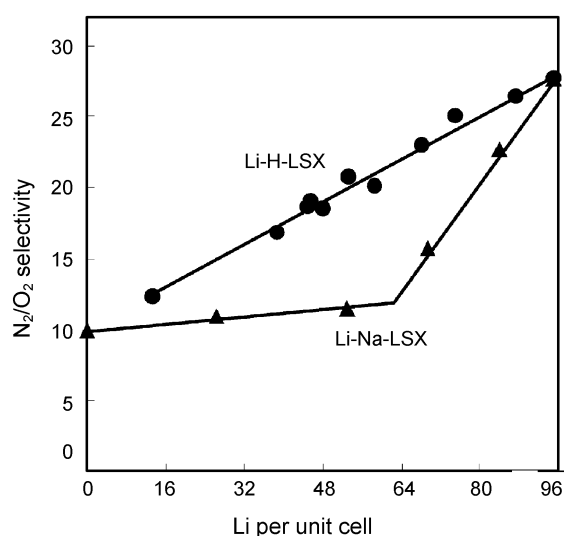


Figure 5. Change in N_2/O_2 selectivity by Li content in Li-H-LSX (●) and Li-Na-LSX (▲) at 20 °C. The selectivity was calculated by N_2 adsorbed at 608 torr and O_2 adsorbed at 152 torr.

Li per unit cell in FAU structure, respectively. The unit cell composition of LSX with Si/Al ratio of 1.0 can be described as $M_{96}Al_{96}Si_{96}O_{384}$, where M indicates alkali metals or proton. The numbers of Li and Na per unit cell were calculated from the chemical analyses by ICP. It was confirmed that the (Li+Na)/Al ratio of Li-Na-LSX was almost 1.0. In Li-H-LSX, the amount of nitrogen adsorbed increased linearly with the increase in the number of Li per unit cell. In the region of low Li-exchanged ratio in Li-H-LSX, as indicated with the broken line, crystal structure of LSX had broken significantly. The structure of LSX, which was highly exchanged with ammonium ions, was destroyed easily only by drying at 100 °C. Although the stability decreased with increase in NH_4 -exchanged ratio, the crystal structure of LSX was maintained until it became about 50%.

Figure 5 shows the change in N_2/O_2 selectivity by the number of Li per unit cell. The N_2/O_2 selectivity was calculated by N_2 adsorbed at 608 torr and O_2 adsorbed at 152 torr. The change of the N_2/O_2 selectivity by the number of Li per unit cell was also similar to that of the nitrogen adsorption amount as shown in Figure 4. Especially, the decrease of N_2/O_2 selectivity in Li-H-LSX with decrease in Li content was very small. Therefore, it is considered that introduction of proton to Li-LSX could be effective in suppressing the decrease of the adsorption performance with decrease in Li content.

Figure 6 shows the d_{111} -spacing values calculated from XRD peaks of Li-Na- and Li-H-LSX with various contents of Li. The d_{111} -spacing value of Na-LSX (100% Na-exchanged LSX) was about 14.3 Å, and reduced remarkably by introduction of Li ions in the range with the low content of Li. The reduction in the d_{111} -spacing value, in Li-Na-LSX, became slow above Li/Al ratio of about 1/3. By contrast, in the Li-H-LSX, the d_{111} -spacing value hardly changed with Li content. On the other hand, the d_{111} -spacing value of partially H-exchanged Na-LSX was also reduced, which was

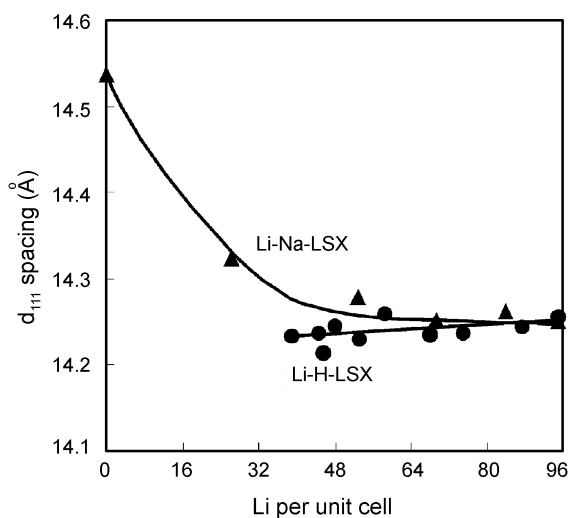


Figure 6. Change in d_{111} -spacing by Li content in Li-H-LSX (●) and Li-Na-LSX (▲).

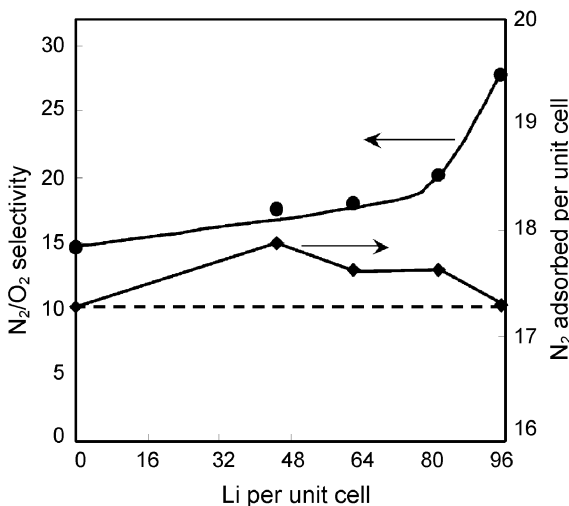


Figure 7. Effect of Li content on N_2/O_2 selectivity (●) and the amount of nitrogen adsorbed (▲) at 20 °C, 760 torr in Li-Ca-LSX.

similar to the effect of Li-exchange. Therefore, probably, H^+ and Li^+ exchange in LSX have the effect on FAU framework being reduced and becoming unstable.

The hypothesis of reference¹² about the position of Li ions contributed to adsorption was well in agreement with an experimental results for the Li-Na-LSX. However, it was hard to understand that the Li ions located site II without structural restrictions did not participate in nitrogen adsorption. The results shown in Figure 6 indicate that the interaction of Li ions and framework of FAU structure affect the adsorption performance of Li-exchanged LSX. In Li-Na-LSX, it was considered due to the interaction with framework that Li ions below Li/Al ratio of about 2/3 did not contribute to adsorption. The influence of proton on the FAU framework structure was similar to that of Li. If the hypothesis¹² about position of Li ions in FAU structure can apply to Li-H-LSX, Li ions located in the site II are also considered to be useful to nitrogen adsorption. Since a lot of

expensive materials like lithium chloride should be consumed in order to obtain the highly Li-exchanged LSX, the consumption of lithium materials could be significantly reducible with these results.

In Li and Ca co-exchanged LSX (Li-Ca-LSX), the amount of nitrogen adsorbed slightly higher than that of Li-LSX and Ca-LSX as shown in Figure 7, and this result was similar to that of reference.¹⁵ Since the nitrogen capacity of Ca-LSX at 760 torr, 20 °C was almost same as that of Li-LSX, there was almost no effect of Li-exchange to Ca-LSX on the amount of nitrogen adsorbed. However, the N_2/O_2 selectivity of Ca-LSX was significantly lower than that of Li-LSX because of the high oxygen adsorption capacity of Ca-LSX as shown in Figure 3. Although the N_2/O_2 selectivity in Li-Ca-LSX was slightly increased with increase in Li content, the selectivity was very low value of about 20 until the number of Li per unit cell reached 80. Therefore, in Li-Ca-LSX, it is considered that the characteristics of Ca ions are more predominant than that of Li ions.

Conclusion

By introducing proton as second cation to Li-LSX, decline in the selective nitrogen adsorption performance accompanying decrease in the Li-exchanged ratio was able to be suppressed. It is considered that the proton in the H-Li-LSX diminished the interaction of Li ions and FAU framework and peculiar adsorption properties by the position of Li ions in the Li-Na-LSX disappeared. Consequently, also in the range with the low content of Li, the H-Li-LSX showed the high performance of selective nitrogen adsorption. Although introducing of Ca ions enlarged the amount of nitrogen adsorbed slightly, the N_2/O_2 selectivity lowered significantly with decrease of Li-exchanged ratio.

Acknowledgement. The author thanks to Dr. Tomoyuki Inui, emeritus professor of Kyoto University, Mr. Hiromi Kiyama, Mr. Haruo Yoshioka and Mr. Hisanao Jo in Air Water Inc. of Japan for helpful advices and discussions.

References

1. Minato, H.; Watanabe, M. *Sci. Pap. Coll. Gen. Educ., Univ. Tokyo* **1978**, 28, 135.
2. Minato, H.; Watanabe, M. *Sci. Pap. Coll. Gen. Educ., Univ. Tokyo* **1978**, 28, 215.
3. Coe, C. G.; Kuznicki, S. M.; Srinivasan, R.; Jenkins, R. J. *Perspectives in Molecular Sieve Science: ACS Symp. Ser.* **1988**, 368, 478.
4. Milton, R. M. *U. S. Patent* 2 882 244, **1959**.
5. McKee, D. W. *U. S. Patent* 3 140 933, **1964**.
6. Chao C. C. *U. S. Patent* 4 859 217, **1989**.
7. Baksh, M. S. A.; Kikkinides, E. S.; Yang, R. T. *Sep. Sci. Technol.* **1992**, 27, 277.
8. Gaffney, T. R. *Current Opinion in Solid State & Material Science* **1996**, 1, 69.
9. Kirner, J. F.; Pa, O. *U. S. Patent* 5 268 023, **1993**.
10. Rege, S. U.; Yang, R. T. *Ind. End. Chem. Res.* **1997**, 36, 5358.
11. Hutson, N. D.; Rege, S. U.; Yang, R. T. *AIChE* **1999**, 45, 724.
12. Yoshida, S.; Ogawa, N.; Kamioka, K.; Hirano, S.; Mori, T.

- Adsorption* **1999**, 5, 57.
13. Yoshida, S.; Hirano, S.; Harada, A.; Nakano, M. *Micropor. Mesopor. Mater.* **2001**, 46, 203.
14. Sherry, H. S. *J. Phys. Chem.* **1966**, 70, 1158.
15. Coe, C. G.; Kirner, J. F.; Pierantozz, R.; White, T. R. *U. S. Patent* 5 152 813, **1992**.
16. Kirner, J. F. *U.S. Patent* 5 268 023, **1993**.
17. Leavitt, F. W. *U.S. Patent* 5 451 383, **1995**.
18. Leavitt, F. W. *U.S. Patent* 5 681 477, **1997**.
19. Klinowski, J.; Ramdas, S.; Thomas, J. M.; Fyfe, C. A.; Hartman, J. S. *J. Chem. Soc., Faraday Trans. 2* **1982**, 78, 1025.
20. Thomas, J. M.; Fyfe, C. A.; Ramdas, S.; Klinowski, J.; Gobbi, G. *C. J. Phys. Chem.* **1982**, 86, 3061.
21. Shen, D.; Bülow, M.; Jale, S. R.; Fitch, F. R.; Ojo A. F. *Micropor. Mesopor. Mater.* **2001**, 48, 211.
-